Role of Extracted Nano-metal Oxides From Factory Wastes In Medical Applications

Nadia Jasim Ghdeeb[1*], Aseel Mustafa AbdulMajeed[1], Asma Hadi Mohammed[2]

[1]*Department of Physics, College Of Science, Mustansyriah University, Baghdad, Iraq*
[2]*Department of Physics, College Of Science, Al-Nahrain University, Baghdad, Iraq*

Abstract

   Nanometal oxides were extracted from cement factories wastes and were employed to proliferate skin cancer cells using MTT (Methyl Thiazolyl Tetraolium) assay. MTT assay results for skin cancer cell line A375,for CaO NPs the best concentration was 200 μg/mL,The viability was reduced to 57.28% while the IC_{50} was (69.66) g/mL for A375 and normal cell WRL68 was significantly higher (231.2 g/mL). The cytotoxicity results of CaO: MgO: Fe_2O_3 NPs, at higher concentrations (200 and 400) μg/mL showed a significant difference. The IC_{50} was (106.4) μg/mL for A375and normal cell WRL68 was significantly higher (173.3) μg/ml CaO:MgO:Fe_2O_3 NPs. The nanometal oxides, calcium oxide (CaO) and the mixture (CaO:MgO: Fe_2O_3) were extracted from wastes of cement factory, and then they were oxidized at a temperature of 400C° for (5) hours. The structural and surface properties of the prepared oxides were characterized by X-ray diffraction patterns,FE-SEM and FTIR. The X-ray data reflected that all the oxides have a polycrystalline cubic structure, with a preferred orientation along (111) for calcium oxide, with a preferred orientation along (002) for calcium oxide: magnesium oxide: iron oxide.

Keywords: CaO and CaO: MgO: Fe_2O_3NPs, crystal structure, morphological, Skin cancer

<div dir="rtl">

دور اكاسيد المعادن النانوية المستخلصة من مخلفات المصانع في التطبيقات الطبية

نادية جاسم غضيب[1]* , اسيل مصطفى عبد المجيد[1] , اسماء هادي محمد[2]

[1]قسم الفيزياء, كلية العلوم, الجامعة المستنصرية, بغداد العراق

[2]قسم الفيزياء , كلية العلوم, جامعة النهرين, بغداد العراق

الخلاصة

   تم استخلاص أكاسيد المعادن النانوية من مخلفات مصانع الاسمنت واستخدمت لعلاج خلايا سرطان الجلد باستخدام فحص MTT (Methyl Thiazolyl Tetraolium). نتائج اختبار MTT لخط خلايا سرطان الجلد A375 ، كان أفضل تركيز لـ CaO NPs هو 200 ميكروغرام / مل ، وتم تقليل الحيوية إلى 57.28٪ بينما كان التركيز النصفي الاقصى للتثبيط

</div>

*Email: nadiajasim127@uomustansiriyah.edu.iq

(IC$_{50}$) 69,66ميكروغرام/مل لـ A375 والخلية الطبيعية WRL68 أعلى بكثير (231.2) مايكروغرام /

مل. أظهرت نتائج السمية الخلوية لـ CaO: MgO: Fe$_2$O$_3$ NPs ، فرقا واضحا عند التراكيز العالية (200

و 400) ميكروغرام / مل . كان التركيز النصفي الاقصى للتثبيط

(IC$_{50}$)106,4ميكروغرام / مل لـ A375 والخلية الطبيعية WRL68 أعلى بكثير (173.3) ميكروغرام /

مل. تم استخلاص اكاسيد المعادن النانوية ,اوكسيد الكالسيومCaO ومزيج

(CaO: MgO: Fe$_2$O$_3$) من مخلفات مصانع الاسمنت ، ثم تم أكسدتها عند درجة حرارة 400 درجة مئوية

لمدة (5) ساعات. تميزت الخصائص التركيبية والسطحية للأكاسيد المحضرة بأنماط حيود الأشعة السينية ،

FE−SEM و FTIR. عكست بيانات الأشعة السينية أن جميع الأكاسيد لها تركيب مكعب متعدد البلورات ،

مع اتجاه مفضل على طول (111) لأوكسيد الكالسيوم ،و اتجاه مفضل على طول (002) لأوكسيد الكالسيوم:

أوكسيد المغنيسيوم: أوكسيد الحديد..

1. Introduction

Wastes are the useless by-product of human activities that physically contain the same substances available in the useful product. Wastes have also been defined as any product or material useless to the producer[1]. It is stated that waste can be classified broadly into three main types according to their physical states: liquid, solid, and gaseous. Several classifications exist in different countries[2, 3]. Nanotechnology is a new promising field with potential applications in domestic, manufacturing, and biomedical products[4] Due to the developing number of utilizations, there is a rising risk of human and environmental exposure to nanomaterials. Their potential toxicological effects are still under investigation, and our actual knowledge of the effects of engineered Nano-sized pollutants on biological systems is still incomplete[5, 6]. Nanotechnology applications in drugs and microbial science have been promising to overcome resistance in infectious diseases. Various antibacterial agents, particularly nanoparticles such as metal and metal oxide, have been applied by researchers against various bacteria[7]. Nanoparticles are much more active than larger-sized particles because of their much higher surface area. They also exhibit unique physical and chemical properties [8-10]. Several types of metal and metal oxide nanoparticles such as silver (Ag), silver oxide (Ag$_2$O), titanium dioxide (TiO2), zinc oxide (ZnO), gold (Au), calcium oxide (CaO), silica (Si), copper oxide (CuO), and magnesium oxide (MgO) have been known to show antimicrobial activity [7]. Metal or metal ions are also essential elements for the human body and play a role in over 300 enzyme reactions[11, 12]. Skin chiefly contains two significant layers, the epidermis and the dermis. The epidermis layer is the deepest layer of the skin that is comprised of melanocytes, keratinocytes, Merkel cells, and Langerhans cells[13]. Any irregularity in this layer leads to numerous kinds of skin insults, and cancer is one of them. In general, skin cancer is extensively partitioned into two significant sorts: melanoma (tumors arising from melanocyte dysfunction) and non-melanoma skin cancers (arising from cells derived from the epidermis)[14]. Melanoma happens because of abnormal proliferation of human melanocytes; containing cells, including 90%, 5%, and 1% in the skin, eyes, and intestine, individually.[15, 16]. When contrasted with other skin affronts, melanoma accounts just for 1% of all skin malignant tumors. Despite late advances in therapeutic approaches, melanoma is still the most aggressive skin cancer, showing just 15-20% of five-year endurance rate[17, 18]. Non-melanoma skin cancer (NMSC), caused by hereditary and environmental factors, represents around 95% of skin cancer[19, 20]. Usually, nonmelanoma skin cancer includes numerous other cancerous sorts; however, these sorts are fundamentally partitioned into two primary subtypes: cutaneous squamous cell carcinoma (SCC), and basal cell carcinoma (BCC);they make up almost 99% of all non-melanoma skin cancers (NMSCs)[21]. Numerous studies have suggested that the occurrence rate of NMSC has been augmented by 3–8% worldwide yearly since 1960, and it is 18–20 times higher than that of

melanoma[22, 23]. Men are more in danger of NMSC than women. The risk of progression of NMSC relies upon genotypic, phenotypic, and environmental factors[24]. In light of the rising prevalence of skin tumors, and the difficulties of wasteful medication conveyance frameworks, it is essential to surge the possible methods to avert or cure the disease.

The aim of this research is to extract metals oxcide(CaO and CaO:MgO:Fe2O3 NPs). from factory waste of Kufa cement factory to be used in multiple applications, including cancer treatment.

2. Materials and Methods
2.1. Preparation of CaO and CaO: MgO: Fe2O3 NPs

Calcium was extracted from cement residues of Kufa cement factory using hydrofluoric acid at a concentration of 48%. Several cement residues were placed in a plastic container, and hydrofluoric acid was added and left for 12 hours; then the mixture was washed with distilled water more than ten times and left to dry. A white powder resulted with calcium element. The calcium was oxidized to obtain calcium oxide by placing it in the oven at a temperature of 400 °C for 5 hours.

The mixture of calcium oxide, magnesium oxide, and iron oxide, CaO:MgO:Fe2O3, was obtained from cement waste by heating the powder obtained 12 hours after placing the waste in hydrofluoric acid in an oven at 400 °C for two hours.
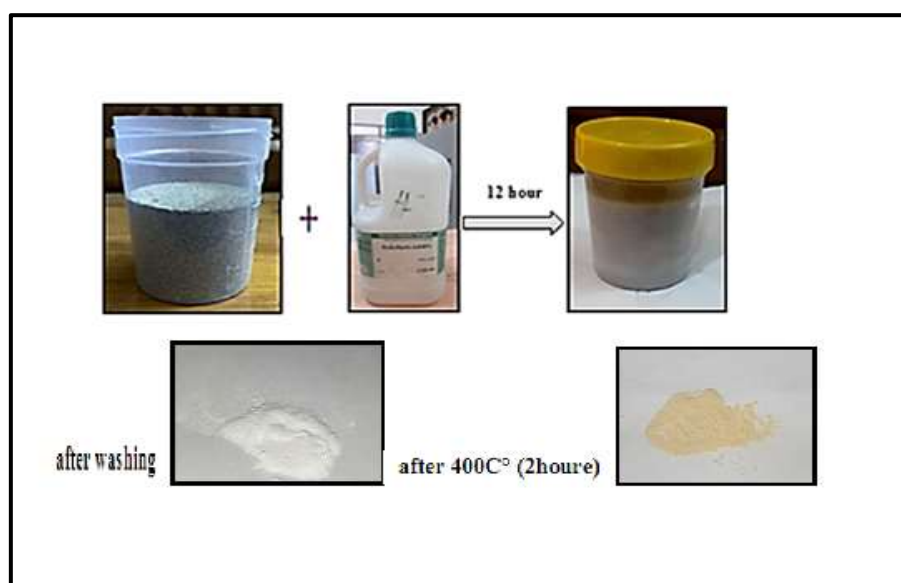
Figure 1: Steps of preparation process of CaO and CaO: MgO: Fe2O3 Nps from cement waste factory

2.2. A375 cell line

Human melanoma (A375) cells were supplied by department of Pharmacology/ Faculty of Medicine, Centre for Natural Product Research and Drug Discovery, University of Malaya. A375 cell line is a human melanoma cell line initiated through explant culture of a solid tumor from a 54-year-old female, stored in liquid nitrogen (-196°C) until ready for experimental use. The control (normal) cells were human hepatic cell lines (WRL-68) which exhibited morphology similar to that of hepatocytes and liver primary cultures.

2.3. MTT assay

To determine the cytotoxic effect of (CaO and CaO: MgO: Fe2O3 NPs), the MTT assay was performed using 96-well plates. Cell line were seeded at 1×10^4 cells/well. After 24

hours a confluent monolayer was achieved; cells were then treated(skin cancer) with tested compounds(CaO and CaO: MgO: Fe2O3 NPs). Cell viability was measured after 72 hours of treatment by removing the medium, adding 10 μL of 2 mg/mL solution of MTT and incubating the cells for 4 h at 37 °C. After removing the MTT solution, the crystals remaining in the wells were solubilized by the addition of 100 μL of DMSO (Dimethyl Sulphoxide) followed by 37 °C incubation for 5 min. Absorbance was measured using an ELISA reader (Bio-rad, Germany) at a wavelength of 575 nm. Statistical analysis was performed on the optical density readings to calculate the half maximal inhibitory concentration IC_{50} according to the following equation:

$$Viabilitiy(\%) = \frac{optical\ densty\ of\ sample}{optical\ density\ of\ control} \times 100\%.$$

3. Results and Discussion
3.1. Structural properties

Figure (2) shows the XRD patterns of CaO and the mixed CaO: MgO: Fe_2O_3 NPs. All the peaks in the XRD patterns of the of the CaO and the mixture of CaO:MgO:Fe_2O_3 NPs can be indexed to the cubic crystal system that matched the ASTM (American Standards for Testing Materials) card of CaONPs (JCPDS card no. 37-1497,30-0794,39-1346), respectively. Several peaks can be noted along the (200), (220), and (222) planes at 2θ of 37.32°, 53.68° and 68.64°, respectively, as matched with the ASTM (American Standards for Testing Materials) card of CaO (37-1497). Our results agree with other researches[25, 26] the (220) plane at 47.02° was also reported by Balaganesh et al[27]. From Figure (2), it is clear that the mixture of CaO: MgO: Fe2O3 NPs occupied all the peaks as matched with the ASTM card of CaO, MgO. Fe_2O_3NPs have preferential orientation along(002) at 29.64°; this matched the results of Tomah and Fadhil[28].The crystallite size was estimated from the XRD pattern using Scherer's equation[29].

$$D = \frac{0.9\lambda}{\beta cos\theta} \qquad \ldots \ldots \ldots \ldots \ldots. (1)$$

Where: λ is the X-ray wavelength of Cu Kα Radiation (1.54 °A), θ is the Bragg diffraction angle, and β is the FWHM of the discrete diffraction peak. The crystal size corresponding to the highest peak observed in the XRD pattern was found to be 34.756, 20.277 nm for CaO and CaO: MgO: Fe_2O_3 NPs, respectively.
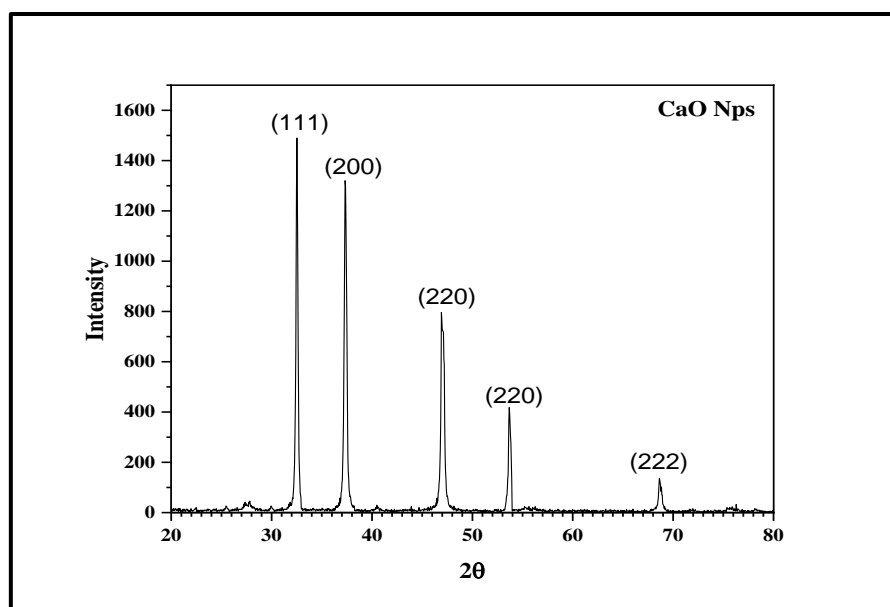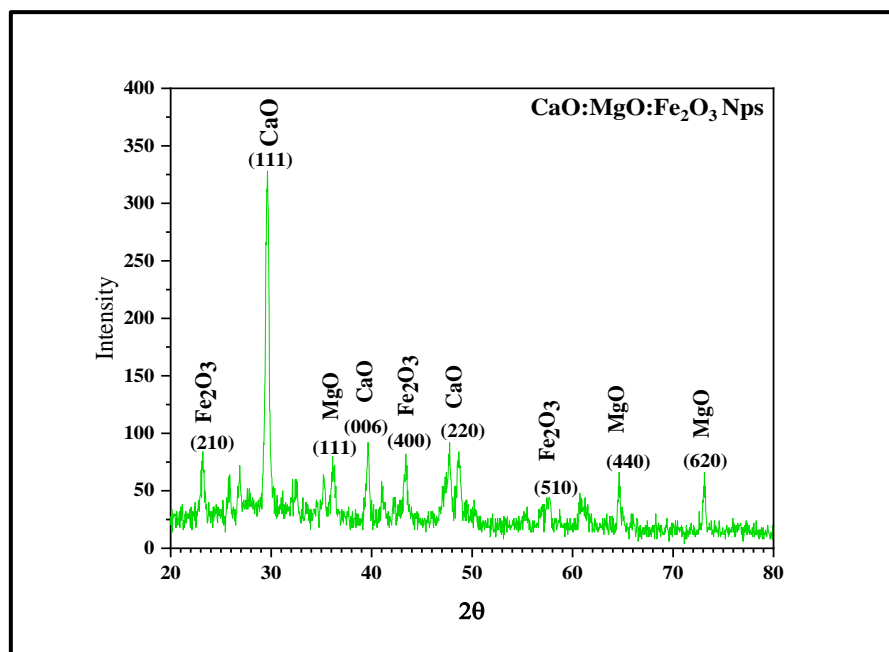
Figure 2: XRD patterns of CaO and CaO: MgO: Fe$_2$O$_3$ NPs

Table 1: The obtained result of the XRD for CaO and CaO: MgO: Fe2O3 NPs

sample	2θ stand (deg.)	2θ Exp. (deg.	FWHM (rad)	Miller indices (h k l)	D(nm)
CaO	32.203	32.52	0.004155	(111)	34.756
	37.346	37.32	0.003885	(200)	37.668
	47.568	47.02	0.003846	(220)	39.292
	53.854	53.68	0.003844	(220)	40.415
	67.373	68.64	0.004091	(222)	41.051
CaO: MgO: Fe$_2$O$_3$	29.756	30.04	0.007073	(111)	20.277
	36.936	36.12	0.007435	(111)	19.615
	39.276	39.6	0.005658	(006)	26.043
	43.284	43.36	0.007010	(400)	21.282
	47.568	47.68	0.006213	(220)	24.397
	56.106	56.88	0.002792	(510)	56.478
	64.526	64.56	0.004653	(440)	35.248
	73.327	73.04	0.003490	(620)	49.436

3.2 Field Emission Scanning Electron Microscope:

Figure (3) shows the energy dispersive X-ray for the cement waste. It can be observed from the figure that the waste contains many elements such as calcium, silicon, chlorine, potassium, iron, sulfur, magnesium, carbon, oxygen and aluminium. Calcium was of the highest percentage among the elements, followed by silicon, sulfur, potassium and the rest. Figure (4) shows the EDX of the cement factory waste after adding hydrofluoric acid (HF) for 12 hours, and after washing well with distilled water, the figure shows that only calcium and fluorine remained after washing.

Figure (5) shows the energy dispersive X-ray of the cement factory waste after adding hydrofluoric acid for the same period as above and with heat treatment for 2 hours at a temperature of 400C$^{\circ}$.

Figure (6) shows the SEM and EDX images of the individual samples of CaO and the mixed CaO: MgO: Fe2O3 NPs synthesized by extraction method using HF acid to obtain calcium oxide and the mixture.

Figure (6a) shows that the grain size of CaO NPs ranged between (48.77-87.57) nm. In addition, CaO NPs were well dispersed. The synthesized CaO NPs were agglomerated forming larger clusters. Figure (6b) shows that the diameters of CaO: MgO: Fe_2O_3 NPs ranged between (81.19-88) nm. To determine the proportions of elements in compounds, energy-dispersive X-ray analysis was used. In this study, it was used to show the presence of CaO NPs, and the mixed sample CaO: MgO: Fe_2O_3 Nps in a certain proportion. The analyses were reported in same patterns as shown in Figure (6a) for CaO NPs and (b) for CaO: MgO: Fe_2O_3 NPs under the EDX spectrum of the study.
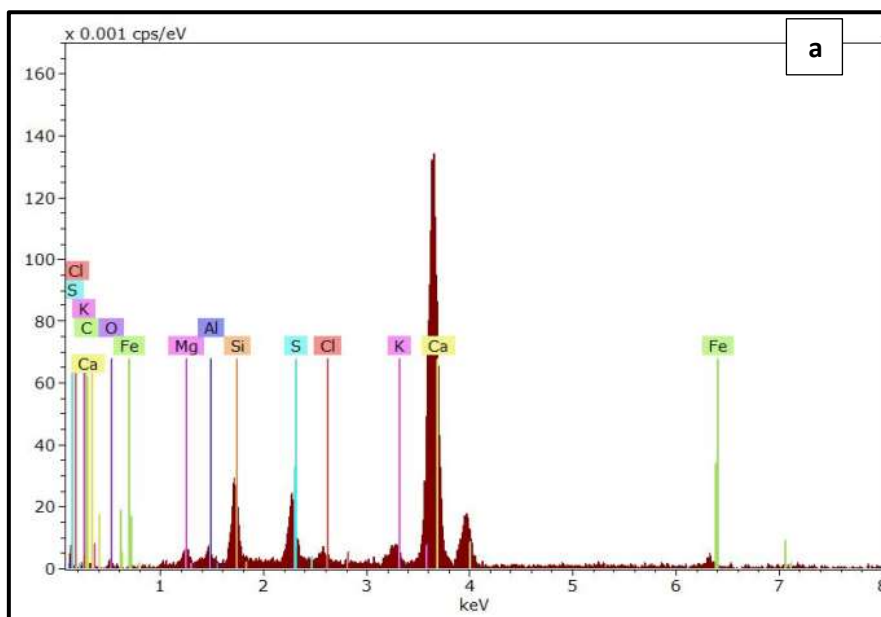
Figure 3:Energy Dispersive X-ray (EDX) of the cement waste
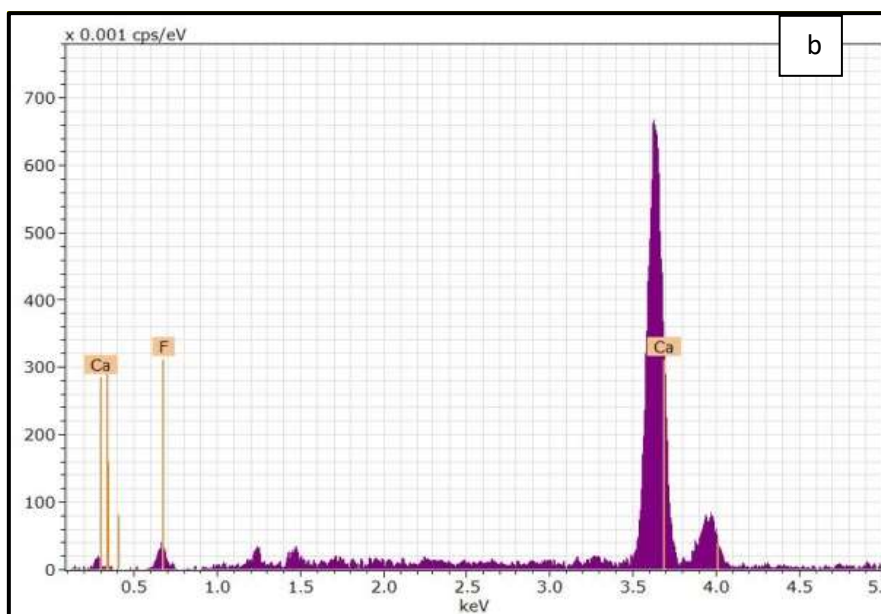
Figure 4: Energy Dispersive X-ray (EDX) of the cement waste after adding hydrofluoric acid
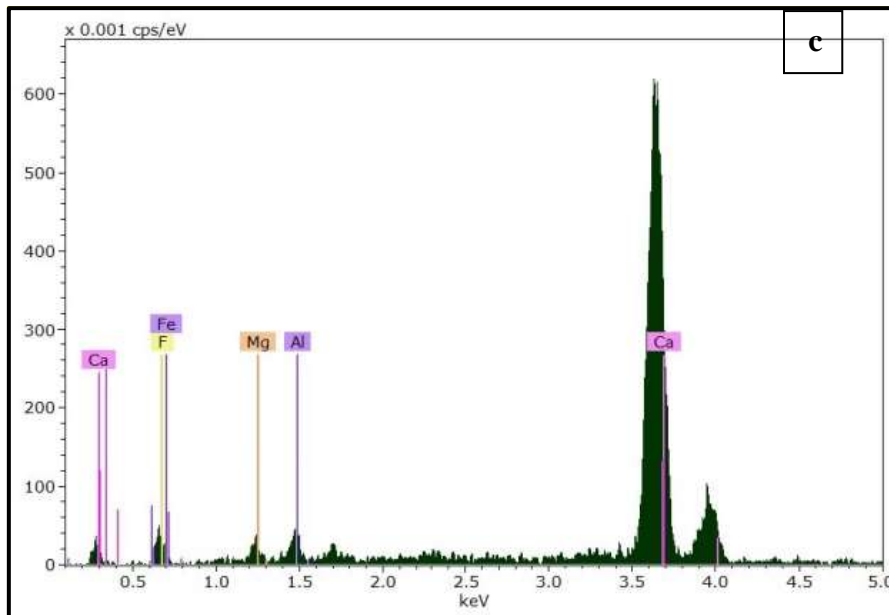
Figure 5: Energy Dispersive X-ray (EDX) of the cement waste after adding hydrofluoric acid and the heat treatment
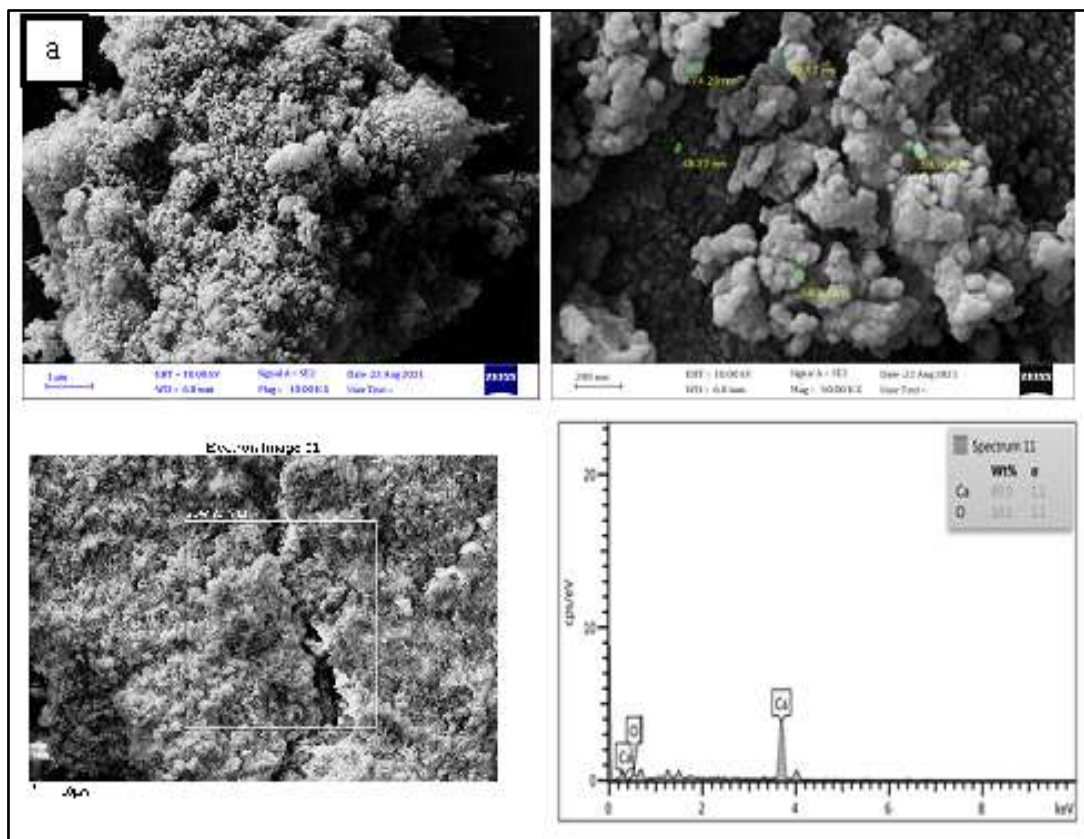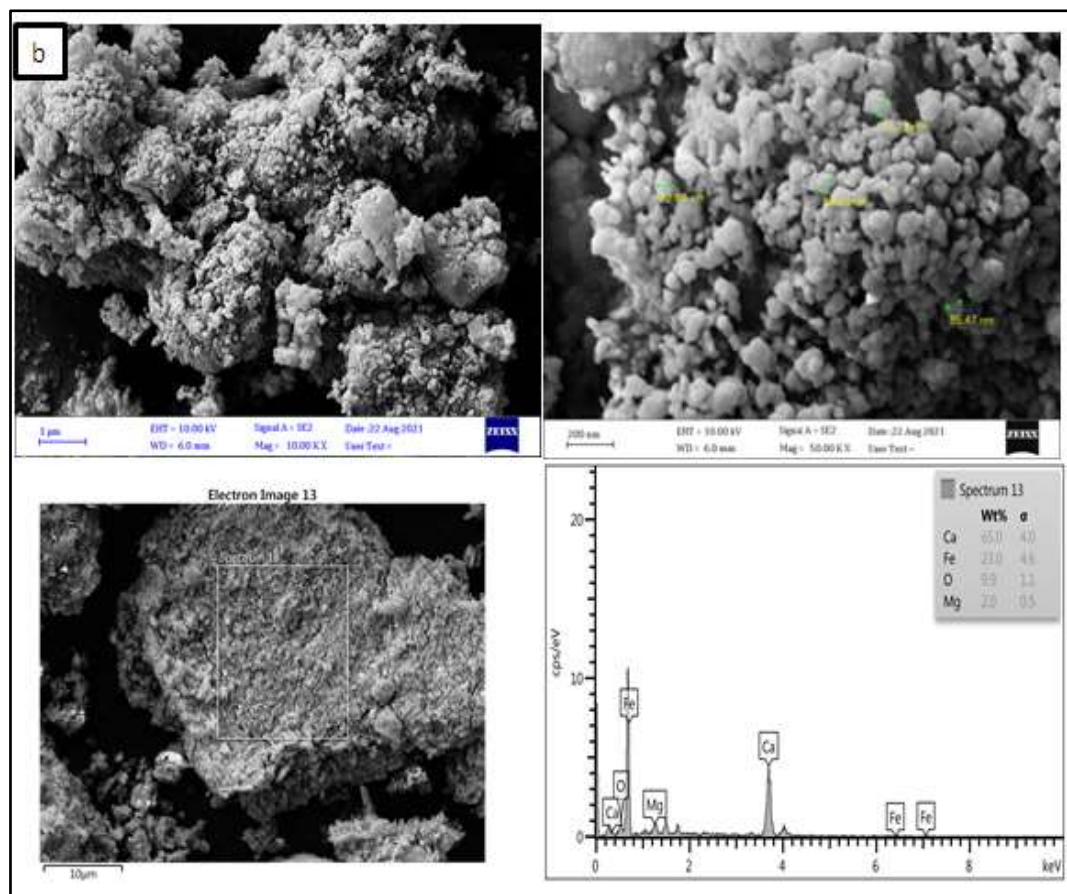
Figure 6: FE-SEM images of CaO and CaO: MgO: Fe2O3 NPs

3.3. Fourier transform infrared spectroscopy (FTIR) analysis

Fourier transform infrared (FTIR) spectroscopy is an essential tool for observation of functional groups; it was employed in this work to characterize the different functional groups, which are involved in the reduction of the stabilization of the prepared CaO and the mixed sample of CaO: MgO: Fe_2O_3 NPs powders. The FTIR spectrum for CaO is shown in Figure (7a). FTIR analysis expressed visible bands at 3452.23, 1173.43, 1123.89, 738.78, and 638.45 cm^{-1}. The band found at 3452.23cm^{-1} can be assigned to stretching of the O-H[26]]. The two peaks appeared between 1173.43-1123.89cm^{-1} refers to C-O stretching vibration[26, 30] The peaks at 638.45 cm^{-1}refers to C-H out of plane bending, and the strong band observed at 718.78 cm^{-1} is due to the(Ca-O) bond. These results agree with those of Mmusiet al[31] and Jalua et al[32] Figure (7b)shows the FTIR spectrum of the synthesized mixture of CaO :MgO: Fe_2O_3 NPs; the band at 3441.72cm^{-1} can be assigned to the stretching of the O-H; 1121.98 cm^{-1} refers to C-O stretching vibration; the peaks between729.25and 622.62 cm^{-1}refers to C-H out of plane bending. The appearance of the peak at 564 cm^{-1} was due to the vibrational intrinsic stretching of metal oxygen bond vibrations (Fe-O)[33]
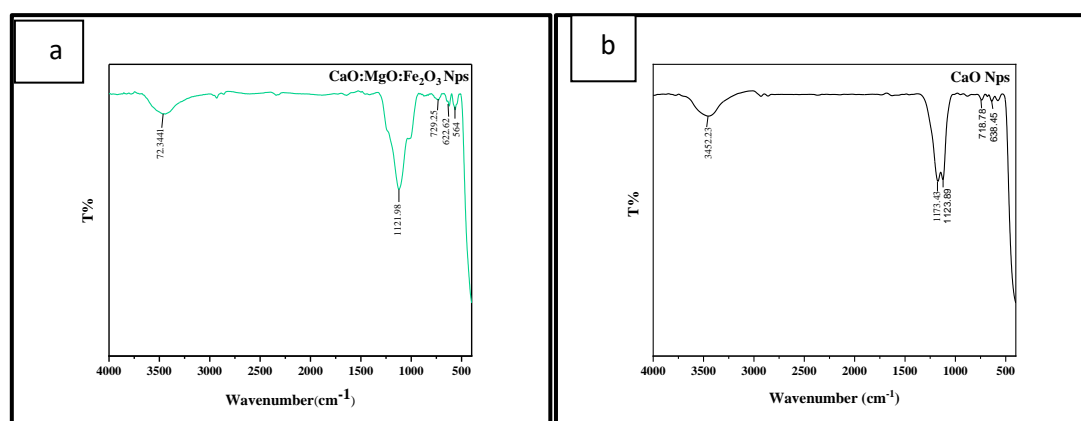
Figure 7: Fourier transform Infrared (FT-IR) analysis of CaO and CaO: MgO: Fe$_2$O$_3$ NPs

3.4. Cell viability (MTT Assay):

To check the cytotoxicity of the individual samples CaO and the mixed CaO: MgO: Fe$_2$O$_3$NPs on the human melanoma A375 cell line (in Vitro), (1×10^5 ml^{-1}) cells per well, in their exponential growth phase, were incubated for 24 hours with different concentrations CaO and CaO: MgO: Fe2O3 NPs. The cell viability was estimated as a percentage of the control (100 % cell viability was investigated by MTT assay).

Cytotoxicity results of human melanoma A375 cell line viability after 72 hours of treatment with various concentrations (6.25 to 400μg/Ml) of CaO and CaO: MgO: Fe2O3 NPs are shown in Figures (8). All results indicated a decrease in cell viability in a dose-dependent manner and both CaO NPs and CaO: MgO: Fe2O3 NPs solutions resulted in a significant reduction in the survival rate of A375cells in dose dependence ($P < 0.0001$). For CaO NPs, The best concentration was 200 μg/mL, where the viability was reduced to 57.28% at a concentration of (6.25and 12.5) μg/Ml.There was no significant difference in viability of A375 carcinoma. While the IC50 was (69.66) μg/mL for A375 and for normal cell WRL68 was significantly higher (231.2 μg/mL). Table (2) shows the viability (mean ± standard deviation (SD) of the CaO NPs.

The cytotoxicity results of the mixed CaO: MgO: Fe$_2$O$_3$ NPs are shown in Figure (8b) and Table (3). There was no significant difference between A375carcinoma and normal cell human hepatic cell lines (WRL68) for the concentrations of (6.25, 12.5, 25, and 50) μg/mL of CaO: MgO: Fe$_2$O$_3$ NPs, at higher concentrations (200 and 400) μg/Ml, a significant difference was observed. The half maximal inhibitory concentration (IC$_{50}$) was (106.4) μg/mL for human melanoma A375 cell line and normal cell WRL68 was significantly higher at (173.3) μg/mL for CaO: MgO: Fe$_2$O$_3$ NPs.

From the above results, it was found that CaO and CaO: MgO: Fe$_2$O$_3$ NPs extracted from cement factories proved their effectiveness in inhibiting skin cancer cells, especially the CaO: MgO: Fe$_2$O$_3$ NPs, where the percentage of inhibition of cancer cells was approximately 70%.

Nanomaterials attack cells by penetrating the cell wall, and as a result, the permeability of the cell membrane changes and its permeability increases. This makes difficult to control the entry of substances through the cytoplasmic membrane, resulting in cell death.

Table 2: Viability (mean ± standard deviation (SD) of CaO NPs

Concen. (µg/mL)	A375		WRL68	
	Mean	**±SD**	**Mean**	**±SD**
400.00	67.51	2.79	77.28	3.65
200.00	57.28	3.29	86.03	0.85
100.00	67.62	2.70	92.13	1.56
50.00	90.97	1.98	96.18	1.25
25.00	94.56	2.81	96.95	1.14
12.50	96.88	0.99	94.91	2.20
6.25	96.10	1.71	96.10	0.48

Table 3: Viability (mean ± standard deviation (SD) of CaO: MgO: Fe_2O_3 NPs

Concen. (µg/mL)	A375		WRL68	
	Mean	**±SD**	**Mean**	**±SD**
400.00	33.40	3.31	68.09	6.80
200.00	50.95	8.76	77.08	5.52
100.00	72.83	1.54	93.60	2.10
50.00	95.45	0.88	95.33	1.18
25.00	97.15	1.35	95.22	0.82
12.50	95.87	3.28	95.95	1.03
6.25	95.99	0.96	95.95	0.20
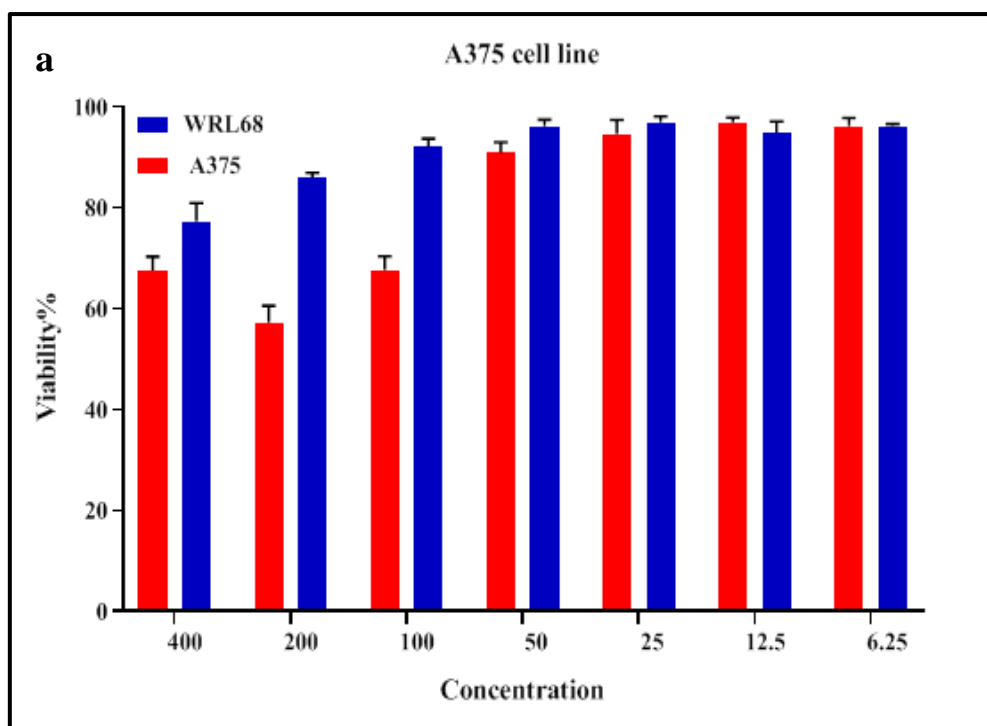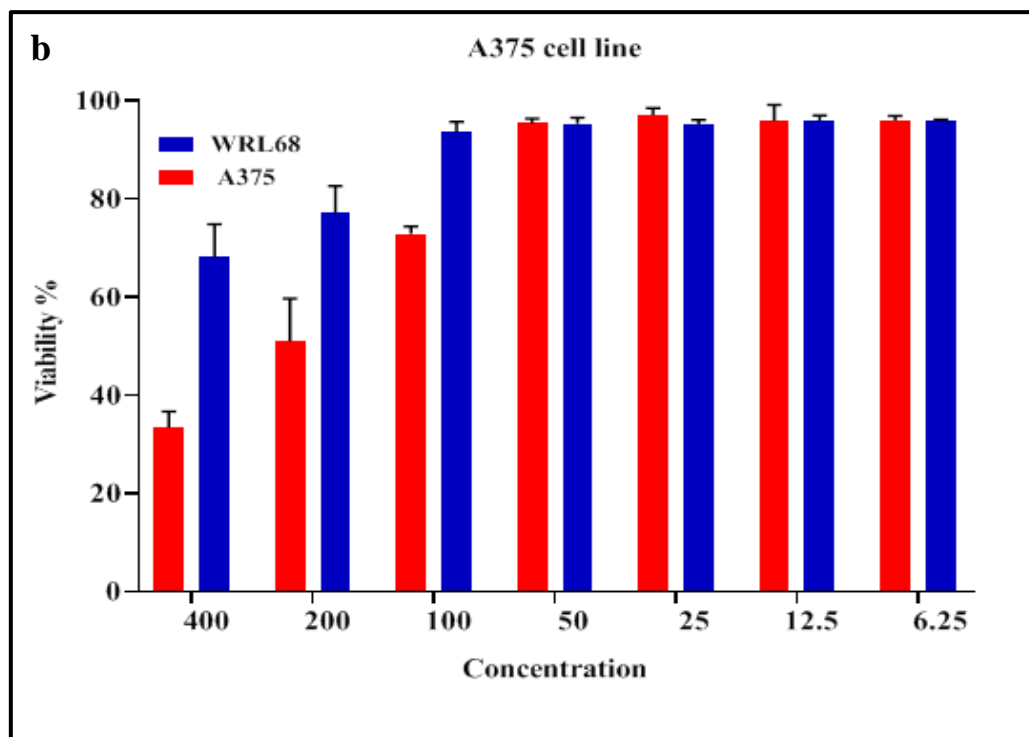
Figure 8: Cell Viability rate of (a) CaO, (b) CaO: MgO: Fe2O3 NPs. A375 cell line

4. Conclusion

Calcium oxide (CaO) and the mixture (CaO: MgO: Fe_2O_3) were successfully extracted from factory wastes. The structural tests showed that all the oxides have a polycrystalline cubic structure. FESEM showed the morphology of CaO NPs and CaO: MgO: Fe2O3 NPs. The average diameter of CaO and the mixed CaO: MgO: Fe2O3 NPs were around (64.08,84.2) nm, respectively. These oxides showed good effectiveness, especially the mixture, where the percentage of inhibition of cancer cells was approximately 70%.

References

[1] E. A. J. Baird, "The Concept of Waste and Waste Management," 2016.

[2] N. Dixon, & Jones, D. R. V, "Engineering properties of municipal solid waste," *Geotextiles & Geomembranes*, vol. 23, pp. 205-233, 2005, doi: https://doi.org/10.1016 /j.geotexmem. 2004.11.002.

[3] A. Demirbas, "Waste management, waste resource facilities, and waste conversion processes," *Energy Conversion & Management*, vol. 52, pp. 1280-1287, 2011, doi: https://doi.org /10.1016/j.enconman.2010.09.025.

[4] Z. L. Peralta-Videa JR, Lopez-Moreno ML, de la Rosa G, and G.-T. J. Hong J, "Nanomaterials and the environment," *J Hazard Mater*, vol. 1, pp. 1-15, 2011.

[5] y. Saud Alarifi , Daoud Ali,y, Ankit Verma, Saad Alakhtani, and Bahy A. Ali "Cytotoxicity and Genotoxicity of Copper Oxide Nanoparticles in Human Skin Keratinocytes Cells," *International Journal of Toxicology*, vol. 4, pp. 296-307, 2013.

[6] F. M. Skocaj M, Petkovic J, Novak S, "Titanium dioxide in our everyday life," *Radiol Oncol*, vol. 4, pp. 227-247, 2011.

[7] M. A. Dizaj SM, Jafari S, Khezri K, Adibkia K, "Antimicrobial activity of carbon-based nanoparticles," *Advanced pharmaceutical bulletin*, vol. 5, pp. 11-19, 2015.

[8] B. F. F. Mirhosseini M, "Preparation of ZnO-Polystyerne Composite Films and Investigation of Antibacterial Properties of ZnOPolystyerne Composite Films," *Iranian Journal of Pathology*, vol. 2, pp. 99-106, 2014.

[9] Z. S. El-Nahhal I, Kodeh F, Selmane M, Genois I, Babonneau F, "Nanostructured copper oxide-cotton fibers: synthesis, characterization, and applications," *International Nano Letters,* vol. 3, 2012.

[10] R. B. Jones N, Ranjit KT ,Manna AC, "Antibacterial activity of ZnO nanoparticle suspensions on a broad spectrum of microorganisms," *FEMS microbiology letters*, vol. 1, pp. 71-76, 2008.

[11] W. M, *editor Anti-Microbial Porcelain Enamels. 62nd Porcelain*

[12] Enamel Institute Technical Forum," Ceramic Engineering and Science Proceedings, vol. 21, 2000.

[13] S. HH, "Understanding zinc: recent observations and interpretations," *The Journal of laboratory and clinical medicine,* 3, pp. 322-327, 1994..

[14] L. WD, "Anatomy of the skin and the pathogenesis of nonmelanoma skin cancer," *Facial Plastic Surgery Clinics*, vol. 3, pp. 283–289, 2017.

[15] K. B. Esteva A, Novoa RA, Ko J, Swetter SM, Blau HM, "Dermatologist-level classification of skin cancer with deep neural networks," *nature,* vol. 9, pp. 115-118, 2017.

[16] W. C. Gray-Schopfer V, Marais R, "Melanoma biology and new targeted therapy," *Nature,* pp. 851–857, 2007.

[17] S. P. Pópulo H, Lopes JM, "Insights into melanoma: targeting the mTOR pathway for therapeutics.," *Expert opinion on therapeutic targets* vol. 7, pp. 689–705, 2012.

[18] M. K. Siegel RL, Jemal A, "Cancer statistics," *cancer journal for clinicians*, vol. 1, pp. 7-30, 2016.

[19] S. AC. "Cancer Facts & Figures." (accessed. P. G. Didona D, Bottoni U, Cantisani C, "Non melanoma skin cancer pathogenesis overview," *Biomedicines*, vol. 1, pp. 1-6, 2018.

[20] C. E, Al-Niami F. "Skin cancer," *Medicine*, vol. 7, pp. 431–434, 2017.

[21] O. C. Green AC, "Cutaneous squamous cell carcinoma: an epidemiological," *Br J Dermatol* vol. 2, pp. 373–381, 2017.

[22] L. A. Apalla Z, Sotiriou E, Lazaridou E, Ioannides D, "Epidemiological trends in skin cancer," *Dermatology practical & conceptual*, vol. 2, pp. 1-, 2017.

[23] K. R .Eide MJ, Johnson D, Long JJ, Jacobsen G, Asgari MM, "Identification of patients with nonmelanoma skin cancer using health maintenance organization claims data, " *Am J Epidemiol* vol. 1, pp. 123-128, 2010.

[24] O. C. Green AC, "Changing patterns in incidence of non-melanoma skin cancer," *Epithelial Cell Biol*, vol. 1, pp. 47-51, 1992.

[25] V. S. Suresh Kumar, Jatindra Kumar Pradhan, Sanjay Kumar Sharma, Prem Singh, Jatinder Kumar Sharma, "Structural, Optical and Antibacterial Response of CaO Nanoparticles Synthesized via Direct Precipitation Technique," *Nano Biomed. Eng., 2021,* vol. 13, pp. 172-178, 2021.

[26] F. B. Zahra Mirghiasi , Esmaeel Darezereshki , Esmat Esmaeilzadeh, " Preparation and characterization of CaO nanoparticles from Ca(OH)2 by direct thermal decomposition method", vol. 20, pp. 113–117, 2014.

[27] R. S. A.S. Balaganesh, R. Ranjithkumar, B. Chandarshekar "Synthesis and Characterization of Porous Calcium Oxide Nanoparticles (CaO NPS " *International Journal of   Innovative Technology and Exploring Engineering*, vol. 8, pp. 312-314, 2018.

[28] A. K. F. W.O.Toamah, "Preparation of nanoparticles from CaO and use it for removal of chromium (II), and mercury (II) from aqueous solutions," *IOP Conf. Series: Journal of Physics,* vol. 1234, pp. 1-9, 201 ,doi: 10.1088/1742-6596/1234/1/012086 .

[29] E. K. j. Nadia J.Ghdeeb, Noha H. Harb, Nisreen.Kh.abdalameer, "Studying Structural, Morphological And Optical Properties of Cadmium Oxide," *Advances In Natural And Applied Sciences*, vol. 12, pp. 21-25, 2018.

[30] S. K. A. Dhupar, V. Sharma, "Mixed structure Zn(S,O) nanoparticles: Synthesis and characterization," *Materials Science Poland*, vol. 37, pp. 230-237, 2019.

[31] S. O. Keene Carlvin Mmusi , and Florence Nareetsile, "Comparison of CaO-NPs and Chicken Eggshell-DerivedCaOin the Production of Biodiesel from(Mongongo) Nut Oil," *Hindawi Journal of Chemistry*, vol. 2021, 2021.

[32] T. A. C. Reta G. Jalua , Dr. Ramachandran Kasirajanc "Calcium oxide nanoparticles synthesis from hen eggshells for removal of lead) Pb(II)) from aqueous solution," Environmental Challenges, vol. 4, 2021.

[33] M. S. A. Abdulaziz Alangari , 2Ayesha Mateen , Mohd Abul Kalam , Abdullah Alshememry ,Raisuddin Ali ,Mohsin Kazi ,Khalid M. AlGhamdi ,and Rabbani Syed, "Iron Oxide Nanoparticles: Preparation, Characterization, and Assessment of Antimicrobial and Anticancer Activity," Adsorption Science & Technology vol. 2022, pp. 1-9, 2022, doi: https://doi.org/10.1155/2022/1562051.